Supporting information

Title: High performance boronic acid-containing hydrogel for biocompatible continuous glucose monitoring

Qian Dou, [a] Debo Hu,[a] Hongkai Gao,[b] Yongmei Zhang,[b] Ali K. Yetisen,[c,d] Haider Butt,[e] Jing Wang,[a] Guangjun Nie,[*a] Qing Dai[*a]

[a.] Division of Nanophotonics, CAS Center for Excellence in Nanoscience, National Center for Nanoscience and Technology, Beijing 100190, P. R. China.

[b.] The Armed Police General Hospital, Beijing, 100039, China.

[c.] Harvard Medical School and Wellman Center for Photomedicine, Massachusetts General Hospital, 65 Landsdowne Street, Cambridge, Massachusetts 02139, USA.

[d.] Harvard-MIT Division of Health Sciences and Technology, Massachusetts Institute of Technology, Cambridge, Massachusetts 02139, USA.

[e.] University of Birmingham, Birmingham B15 2TT, United Kingdom.

E-mail: daiq@nanoctr.cn, Tel: +86-010-82545720

Figures

Detection limit and resolution of glucose sensor

Gradually increasing the concentration of glucose to obtain the detection limit and resolution of the sensor. It can be seen from the Figure S1, when the glucose concentration increased to 0.02 mM, the frequency decreased by ～3 Hz. It can be seen that the detection limit of the sensor is 0.02 mM. When the concentration interval of glucose was 0.02 mM, the frequency was decreased stably. We can see that the resolution of the sensor is also 0.02 mM.

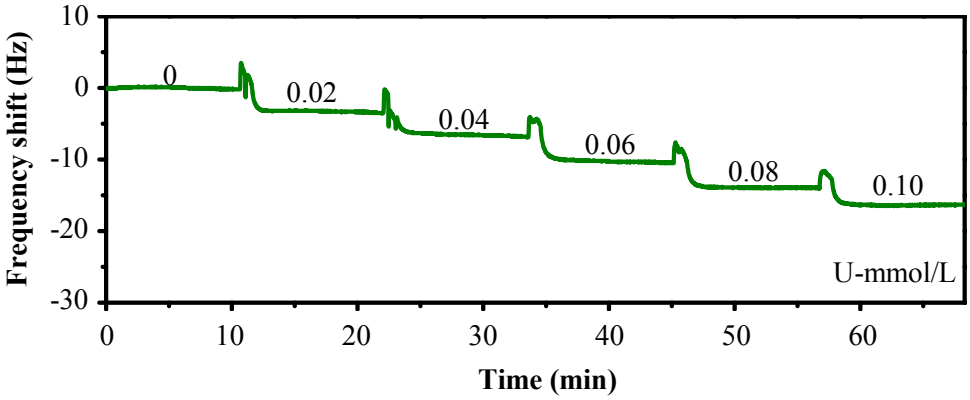

Figure S1. Detection limit and resolution of glucose sensor (pH 7.5)

The relationship between glucose concentration and frequency

To obtain optimal linear fitting between frequency shift and glucose concentration, we performed the fitting in different glucose concentration range. The specific linear figure and equations are shown in Figure S2 and Table S1 at different pH in the ranges of 0.0~9.4 mM and 9.4~33.3 mM.

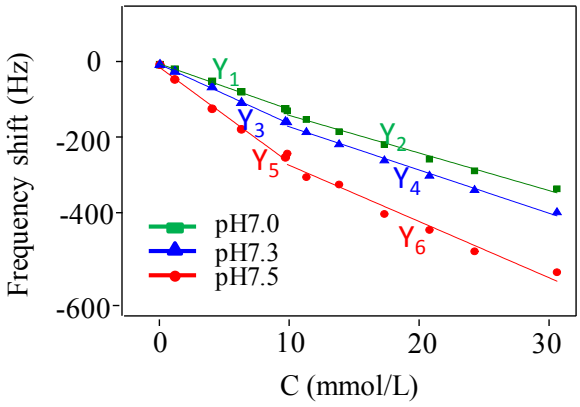

Figure S2. The relationship between glucose concentration and frequency

Table S1. The linear equations

Linear equation	R^2
Y_1=-9.5092*X_1+1.4544	0.9971
Y_2=-7.5181*X_2-28.0212	0.9870
Y_3=-19.8577*X_3-6.2967	0.9934
Y_4=-11.2477*X_4-107.1605	0.9637
Y_5=-12.3826*X_5+0.1219	0.9983
Y_6=-8.6541*X_6-43.2303	0.9921

Implantation experiments

After implantation of the coated chip and control samples (high-density Teflon), there was no significant change in the feeding and activity of the animals. After the operation (Figure S2), local inflammation was observed, characterized by redness and wound inflammation. Inflammation was due to the surgical wound, not the implant materials. One week later, most of the wounds were healed and exhibited no inflammation.

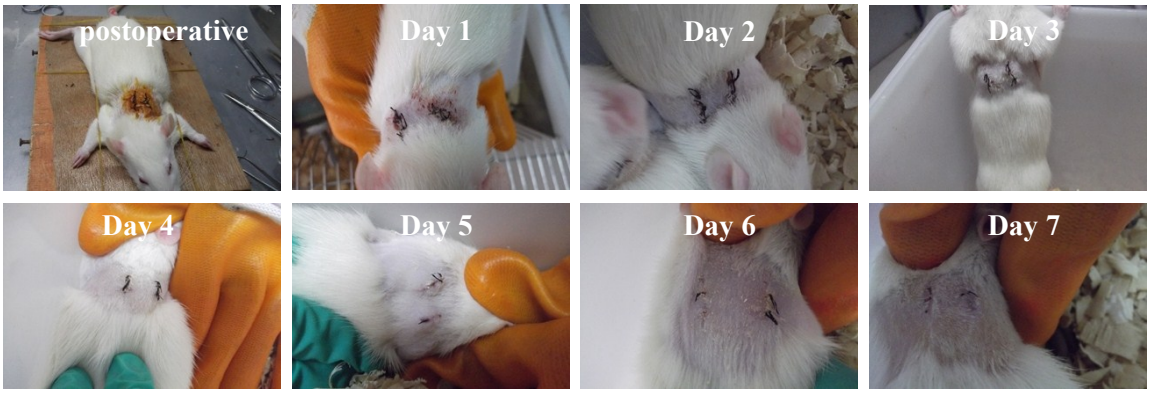

Figure S3. The wound condition of SD rats at different time after implantation

In fact, the implantation experiment lasted for 28 days. Tissues were imaged at fourteen and twenty-eight days post-implantation (Figure S3a and S3b). At fourteen days post-implantation, a small amount of fibrous tissue twined around the implants. At twenty-eight days post-implantation, the implants were all twined around by thicker fibrous tissue (The microscopic images were imaged at the top-right corner in Figure S4a and S4b-Day 28), which exhibited normal fibroblast morphology and

several instances of microvascular generation. Until twenty-eight days post-implantation, six of the hydrogels had fallen off the gold-plate silicon, and two exhibited some shrinkage. All the SD rats´ diet, activities and defecation were normal during implantation. The wounds were all healed and no inflammation at fourteen and twenty-eight days post-implantation (Figure S4c).

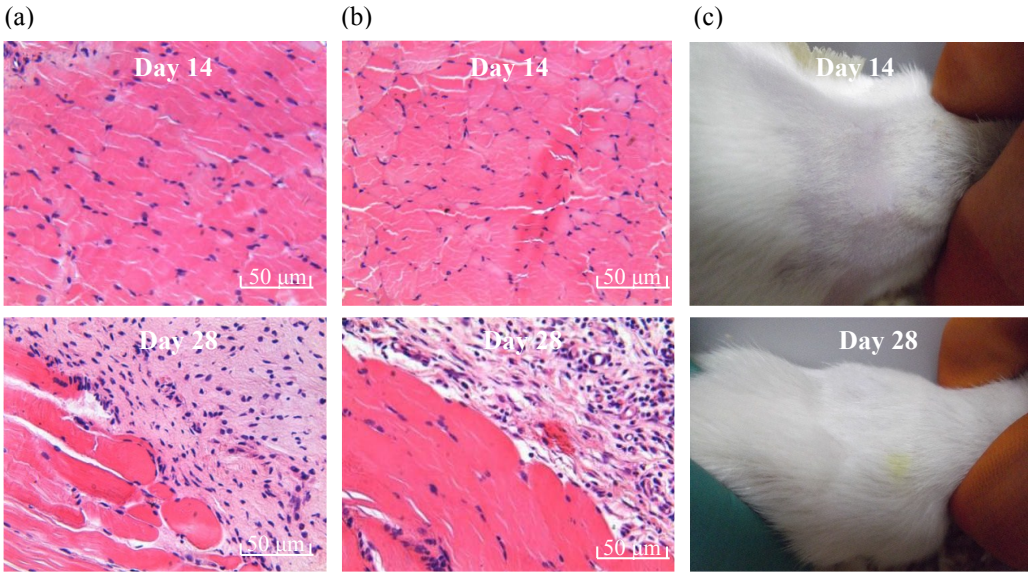

Figure S4a.The animal tissues microscopic images of the control group at different implant time;
Figure S4b.The animal tissues microscopic images of the experiment group at different implant time;
Figure S4c. The wound condition of SD rats at at fourteen and twenty-eight days after implantation